Open Journal of Mathematical Sciences

PSR Press

Article

Peristaltic mechanism of hydromagnetic Jeffrey fluid having variable thermal conductivity and slip conditions

Zahid Amin[1,*], Sobia Tehsin[1] and R. Ahmad [2]

[1] Department of Mathematics, COMSATS University Islamabad, Pakistan.
[2] Graduate School of Mathematics Education, University of Melbourne, 234 Queensberry Street, Melbourne Victoria 3010.
* Correspondence: zahid_amin1064@yahoo.com

Communicated by: Mujahid Abbas
Received: 2 December 2021; Accepted: 21 April 2022; Published: 21 June 2022.

Abstract: In this study, we focus on the slip effects on the peristaltic unsteady flow of magnatohydromagnetic Jeffrey fluid in a flow passage with non-conducting and flexible boundary walls. The effect of the magnetic field with varying thermal conductivity is taken under the influence of heat transfer analysis. The dimensionless system of PDEs is solved analytically, and the obtained results are computed for the temperature, pressure drop, the axial pressure gradient, axial velocity, and then these results are discussed for different values of the physical parameters of our interest. For the stream functions, the contour plots are also obtained which indicates the exact flow behavior within the flow channel, and the effects of the physical parameters on Jeffery fluid within the flow channel are discussed briefly. Our results indicate that the heat transfer coefficient decreases with an increase in thermal slip and velocity slip parameters. Furthermore, it shows that the size of the trapped bolus is greater for the inclined magnetic field as compared to the transverse magnetic field.

Keywords: Jeffrey fluid; Peristaltic flow; Magnetohydrodynamic; Thermal conductivity; Heat transfer; Velocity slip condition; Temperature slip condition.

MSC: 76A05; 35B35; 35D35; 35B40.

1. Introduction

In magnetohydrodynamics some recent studies [1–11] have considered the peristaltic flow of Newtonian and non-Newtonian fluid and investigated the result of magnetic field on them. Stud *et al.,* [12] investigated the interaction of Poiseuille with peristalsis flow. In an asymmetric tube, the effects of peristalsis of viscous fluid are studied by Mekheimer [13].

In the diagnoses of blood circulation and measurements of blood glucose, the study of heat transfer in blood flow plays a vital role. Our normal blood temperature is about 37^0C, but our proteins start damaging when the temperature is increased from 41^0C.In peristalsis flow, the effect of heat transfer has been investigated by many scholars, but a review of heat transfer by Nadeem and Akbar [14] is quite famous in the era of 2003.

Most of the natural physiological fluids like polymer melts, bubbly fluids, hydrocarbons, and many nuclear aggressive materials are based on complicated stress-strain relations as compared to Newtonian fluids. The governing equations of such fluids give challenges to researchers and scholars. The Jeffrey version of the Oldroyed [15–22] is an important example of non-Newtonian fluid models in which time derivative of strain tensor. Peristaltic action of non-Newtonian fluid for small wave amplitude has been described by Raju and Devanathan [23], the long-wavelength peristalsis analysis is performed by Radhakrishnamacharya [24].

In all the studies mentioned above slip effects in presence of variable thermal conductivity have been ignored. Therefore it is of great interest to study the peristaltic mechanism of hydromagnetic Jeffrey fluid having variable thermal conductivity with slip conditions and we did this analysis because of its practical applications in the field of biomedical engineering and food industries in fluid delivery.

2. Mathematical formulation

The unsteady flow of an incompressible hydromagnetic fluid in an asymmetric two-dimensional tube having two walls $\bar{h_1}$ and $\bar{h_2}$ is considered in this study.

The wall geometries as shown in Figure 1 can be expressed as follows:

$$\bar{h}_1(\bar{X},\bar{t}) = \ell_1 + b_1 \cos\left[\frac{2\pi}{\lambda}(\bar{X} - c\bar{t})\right], \tag{1}$$

$$\bar{h}_2(\bar{X},\bar{t}) = -\ell_2 - b_2 \cos\left[\frac{2\pi}{\lambda}(\bar{X} - c\bar{t}) + \theta\right], \tag{2}$$

where ℓ_1 and ℓ_2 are te channel half widths, λ is the wavelength, c is the wave speed, b_1 and b_2 are the amplitudes, $\bar{t}$ is the time, and θ is the phase difference. Furthermore, θ fulfill the condition

$$b_1^2 + b_2^2 + 2b_1 b_2 \cos\theta \leq (\ell_1 + \ell_2)^2. \tag{3}$$

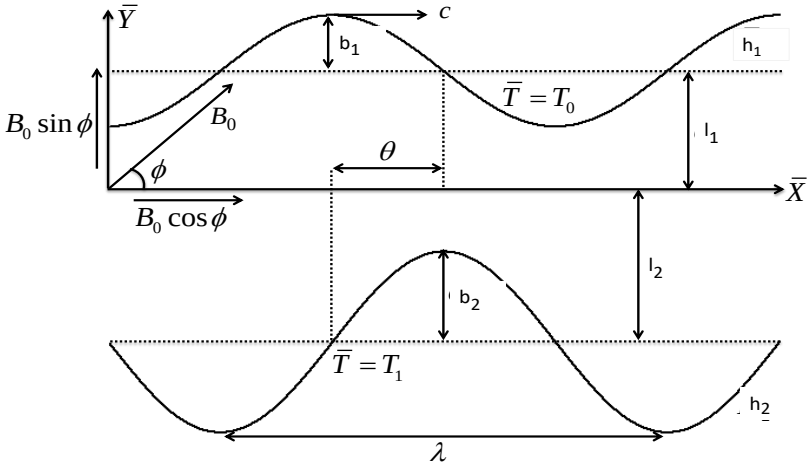

Figure 1. Geometry of the physical model.

It is assumed that T_1 is upper wall temperature and T_2 is the lower wall temperature and T_1 must be less than T_2.

In MHD fluid the governing equations are expressed as

$$\bar{\nabla} \cdot \bar{\mathbf{V}} = 0, \tag{4}$$

$$\rho\left[\frac{\partial \bar{\mathbf{V}}}{\partial \bar{t}} + (\bar{\mathbf{V}} \cdot \nabla)\bar{\mathbf{V}}\right] = \bar{\nabla} \cdot \bar{\mathbf{T}} + \rho\bar{\mathbf{f}}, \tag{5}$$

$$\rho c_p\left[\frac{\partial \bar{T}}{\partial \bar{t}} + (\bar{\mathbf{V}} \cdot \nabla)\bar{T}\right] = -\bar{\nabla} \cdot \bar{\mathbf{q}} + \mathcal{S}_t. \tag{6}$$

In above equation, $\bar{\nabla}$ is the gradient operator, and $\bar{\mathbf{V}} = [\bar{U}(\bar{X},\bar{Y},\bar{t}), \bar{V}(\bar{X},\bar{Y},\bar{t}), 0]$ is the two-dimensional velocity field vector. $\bar{\mathbf{S}}$, $\bar{\mathbf{T}}$, and $\bar{\mathbf{I}}$ are respectively the extra stress tensor for Jeffrey fluid, Cauchy stress tensor and the Identity tensor, $\mathcal{S}_t$ represent the source term, c_p being the specific heat, $\bar{T}$ is the temperature and $\bar{\mathbf{q}}$ is the heat flux vector.

The constitution Jeffrey fluid model equations are

$$\bar{\mathbf{T}} = -\bar{P}\bar{I} + \bar{S}, \tag{7}$$

$$\bar{\mathbf{S}} = \frac{\mu}{1+\lambda_1}[\dot{r} + \lambda_2 \ddot{r}], \tag{8}$$

$$\dot{r} = \mathbf{K} + \mathbf{K}^{\top}, \tag{9}$$

where $\bar{S}$ is extra stress tensor, relaxation time is denoted by λ_1, fluid viscosity by μ, and retardation time by λ_2, $\bar{P}$ is pressure, and $\bar{I}$ is the identity tensor.

The components of extra stress tensor $\bar{\mathbf{S}}$ are

$$\bar{S}_{\bar{X}\bar{X}} = \frac{2\mu}{1+\lambda_1}\left[1+\lambda_2\left(\frac{\partial}{\partial \bar{t}}+\bar{U}\frac{\partial}{\partial \bar{X}}+\bar{V}\frac{\partial}{\partial \bar{Y}}\right)\right]\frac{\partial \bar{U}}{\partial \bar{X}}, \tag{10}$$

$$\bar{S}_{\bar{X}\bar{Y}} = \frac{\mu}{1+\lambda_1}\left[1+\lambda_2\left(\frac{\partial}{\partial \bar{t}}+\bar{U}\frac{\partial}{\partial \bar{X}}+\bar{V}\frac{\partial}{\partial \bar{Y}}\right)\right]\left(\frac{\partial \bar{V}}{\partial \bar{X}}+\frac{\partial \bar{U}}{\partial \bar{Y}}\right), \tag{11}$$

$$\bar{S}_{\bar{Y}\bar{Y}} = \frac{2\mu}{1+\lambda_1}\left[1+\lambda_2\left(\frac{\partial}{\partial \bar{t}}+\bar{U}\frac{\partial}{\partial \bar{X}}+\bar{V}\frac{\partial}{\partial \bar{Y}}\right)\right]\frac{\partial \bar{V}}{\partial \bar{Y}}, \tag{12}$$

and

$$\bar{S}_{\bar{Y}\bar{X}} = \bar{S}_{\bar{X}\bar{Y}},\ \bar{S}_{\bar{X}\bar{Z}} = \bar{S}_{\bar{Y}\bar{Z}} = \bar{S}_{\bar{Z}\bar{X}} = \bar{S}_{\bar{Z}\bar{Y}} = \bar{S}_{\bar{Z}\bar{Z}} = 0. \tag{13}$$

The current density ($\bar{J} = S_e\left[\bar{V}\times \bar{B}_0\right]$) where magnetic field under the negligence of impose electric field and induce electric field represent by $\bar{B}_0 (= [B_0\cos\phi, B_0\sin\phi, 0])$. Thus magnetic body force take the form

$$\bar{J}\times\bar{B}_0 = \left[-S_e B_0^2\left(\bar{U}\sin^2\phi - \bar{V}\cos\phi\sin\phi\right), S_e B_0^2\left(\bar{U}\cos\phi\sin\phi - \bar{V}\cos^2\phi\right), 0\right]. \tag{14}$$

Using above results, Eqs (4)-(6) are modified as

$$\frac{\partial \bar{U}}{\partial \bar{X}}+\frac{\partial \bar{V}}{\partial \bar{Y}} = 0, \tag{15}$$

$$\rho\left(\frac{\partial \bar{U}}{\partial \bar{t}}+\bar{U}\frac{\partial \bar{U}}{\partial \bar{X}}+\bar{V}\frac{\partial \bar{U}}{\partial \bar{Y}}\right) = -\frac{\partial \bar{P}}{\partial \bar{X}}+\frac{\partial \bar{S}_{\bar{X}\bar{X}}}{\partial \bar{X}}+\frac{\partial S_{\bar{X}\bar{Y}}}{\partial \bar{Y}} - S_e B_0^2\left(\bar{U}\sin^2\phi - \bar{V}\cos\phi\sin\phi\right), \tag{16}$$

$$\rho\left(\frac{\partial \bar{V}}{\partial \bar{t}}+\bar{U}\frac{\partial \bar{V}}{\partial \bar{X}}+\bar{V}\frac{\partial \bar{V}}{\partial \bar{Y}}\right) = -\frac{\partial \bar{P}}{\partial \bar{Y}}+\frac{\partial S_{\bar{X}\bar{Y}}}{\partial \bar{X}}+\frac{\partial S_{\bar{Y}\bar{Y}}}{\partial \bar{Y}} - S_e B_0^2\left(\bar{U}\sin\phi\cos\phi - \bar{V}\cos^2\phi\right), \tag{17}$$

$$\rho c_p\left(\frac{\partial \bar{T}}{\partial \bar{t}}+\bar{U}\frac{\partial \bar{T}}{\partial \bar{X}}+\bar{V}\frac{\partial \bar{T}}{\partial \bar{Y}}\right) = \frac{\partial}{\partial \bar{X}}\cdot\left[\bar{\kappa}\left(\bar{T}\right)\left(\frac{\partial \bar{T}}{\partial \bar{X}}+\frac{\partial \bar{T}}{\partial \bar{Y}}\right)\right]+\frac{\partial}{\partial \bar{Y}}\cdot\left[\bar{\kappa}\left(\bar{T}\right)\left(\frac{\partial \bar{T}}{\partial \bar{X}}+\frac{\partial \bar{T}}{\partial \bar{Y}}\right)\right]+\bar{\Phi}_a+\bar{\Phi}_b. \tag{18}$$

In above Eqs (15)-(21), we define the specific heat as c_p, density of the fluid as ρ, and the fluid temperature as $\bar{T}$; whereas, temperature dependent thermal conductivity $\bar{\kappa}(\bar{T})$, the viscous dissipation $\bar{\Phi}_a$, and Joule dissipation $\bar{\Phi}_b$ are defined as follows:

$$\bar{\kappa}\left(\bar{T}\right) = \kappa_0\left[1+\varepsilon_1\left(\bar{T}-T_0\right)\right], \tag{19}$$

$$\begin{aligned}\bar{\Phi}_a =& \frac{\mu}{1+\lambda_1}\left[1+\lambda_2\left(\bar{U}\frac{\partial}{\partial \bar{X}}+\bar{V}\frac{\partial}{\partial \bar{Y}}\right)\right]\\ &\times\left[2\left(\frac{\partial \bar{U}}{\partial \bar{X}}\right)^2+2\left(\frac{\partial \bar{V}}{\partial \bar{Y}}\right)^2+\left(\frac{\partial \bar{U}}{\partial \bar{Y}}\right)^2+\left(\frac{\partial \bar{V}}{\partial \bar{X}}\right)^2+2\left(\frac{\partial \bar{V}}{\partial \bar{X}}\right)\left(\frac{\partial \bar{U}}{\partial \bar{Y}}\right)\right],\end{aligned} \tag{20}$$

and

$$\bar{\Phi}_b = S_e B_0^2\left[\bar{U}\sin\phi - \bar{V}\cos\phi\right], \tag{21}$$

where ε_1 is a constant and κ_0 is the dynamic thermal conductivity.

The unsteady flow in fixed frame $(\bar{X}, \bar{Y}, \bar{t})$ can be treated as steady in the wave frame $(\bar{x}, \bar{y})$ if we define

$$\begin{cases}\bar{u}\left(\bar{x},\bar{y}\right) = \bar{U}\left(\bar{X},\bar{Y},\bar{t}\right) - c,\\ v\left(\bar{x},\bar{y}\right) = \bar{V}\left(\bar{X},\bar{Y},\bar{t}\right),\\ \bar{x} = \bar{X} - c\bar{t},\\ \bar{y} = \bar{Y},\end{cases} \tag{22}$$

where $\bar{u}$ and $\bar{v}$ are the respective components of velocity in $\bar{x}-$direction and $\bar{y}-$directions. Equations (15)$-$(18) after using equations (20)-(22) give

$$\frac{\partial \bar{u}}{\partial \bar{x}}+\frac{\partial \bar{u}}{\partial \bar{y}} = 0, \tag{23}$$

$$\rho\left(\bar{u}\frac{\partial\bar{u}}{\partial\bar{x}}+\bar{v}\frac{\partial\bar{u}}{\partial\bar{y}}\right)=-\frac{\partial\bar{p}}{\partial\bar{x}}+\left(\frac{\partial S_{xx}}{\partial\bar{x}}+\frac{\partial S_{xy}}{\partial\bar{y}}\right)-S_eB_0^2\left(\sin^2\phi(\bar{u}+c)-\frac{\bar{v}}{2}\sin 2\phi\right), \tag{24}$$

$$\left(\bar{u}\frac{\partial\bar{v}}{\partial\bar{x}}+\bar{v}\frac{\partial\bar{v}}{\partial\bar{y}}\right)=-\frac{\partial\bar{p}}{\partial\bar{y}}+\left(\frac{\partial S_{xy}}{\partial\bar{x}}+\frac{\partial S_{yy}}{\partial\bar{y}}\right)+S_eB_0^2\left(-\bar{v}\cos^2\phi+\frac{\bar{u}+c}{2}\sin 2\phi\right), \tag{25}$$

and,

$$\begin{aligned}c_p\left(\bar{u}\frac{\partial\bar{T}}{\partial\bar{x}}+\bar{v}\frac{\partial\bar{T}}{\partial\bar{y}}\right)=&\frac{\partial}{\partial\bar{x}}\cdot\left[\bar{\kappa}\left(\bar{T}\right)\left(\frac{\partial\bar{T}}{\partial\bar{x}}+\frac{\partial\bar{T}}{\partial\bar{y}}\right)\right]+\frac{\partial}{\partial\bar{y}}\cdot\left[\bar{\kappa}\left(\bar{T}\right)\left(\frac{\partial\bar{T}}{\partial\bar{x}}+\frac{\partial\bar{T}}{\partial\bar{y}}\right)\right]+\frac{\mu}{1+\lambda_1}\left[1+\lambda_2\left((\bar{u}+c)\frac{\partial}{\partial\bar{x}}+\bar{v}\frac{\partial}{\partial\bar{y}}\right)\right]\\&\times\left[2\left\{\left(\frac{\partial(\bar{u}+c)}{\partial\bar{x}}\right)^2+\left(\frac{\partial\bar{v}}{\partial\bar{y}}\right)^2\right\}+\left(\frac{\partial(\bar{u}+c)}{\partial\bar{y}}+\frac{\partial\bar{v}}{\partial\bar{x}}\right)^2\right]+S_eB_0^2\left[(\bar{u}+c)\sin\phi-\bar{v}\cos\phi\right].\end{aligned} \tag{26}$$

Introducing the dimensionless variables as follows

$$\begin{cases}x &= \frac{\bar{x}}{\lambda_1},\ y=\frac{\bar{y}}{\ell_1},\mathbf{S}=\frac{\ell_1}{\mu c}\bar{\mathbf{S}},\ u=\frac{\bar{u}}{c},\ v=\frac{\bar{v}}{c},v=-\delta\left(\frac{\partial\psi}{\partial x}\right),\\ T &= \frac{\bar{T}-T_0}{T_1-T_0},\ t=\frac{c\bar{t}}{\lambda_1},\ \kappa=\frac{\bar{\kappa}}{\kappa_0},\ \varepsilon=\varepsilon\left(T_1-T_0\right),\ u=\frac{\partial\psi}{\partial y}.\end{cases} \tag{27}$$

We define dimensionless pressure p, wave number δ, Hartman number M, Brinkman number Br $(=\mathrm{Pr}\times\mathrm{Ec})$, Eckert number Ec, Prandtl number Pr, and Reynolds number Re as follows:

$$\begin{cases}p &= \frac{\ell_1^2}{\mu\lambda_1 c}\bar{p},Br=\frac{\mu c^2}{k_0(T_1-T_0)},M=\sqrt{\frac{S_e}{\mu}}B_0\ell_1,\\ \mathrm{Re} &= \frac{\rho c\ell_1}{\mu},\delta=\frac{\ell_1}{\lambda_1},\ \mathrm{Pr}=\frac{\mu c_p}{\kappa_0},\ \mathrm{Ec}=\frac{c^2}{c_p(T_1-T_0)}.\end{cases} \tag{28}$$

Using Eqs (27) and (28) and adopting the long wavelength procedure, the Eqs (23)-(26) reduce to

$$\frac{\partial p}{\partial x}=\frac{\partial}{\partial y}\left(\frac{1}{1+\lambda_1}\frac{\partial^2\psi}{\partial y^2}\right)-M^2\sin^2\phi\left(\frac{\partial\psi}{\partial y}+1\right), \tag{29}$$

$$\frac{\partial p}{\partial y}=0, \tag{30}$$

and

$$\frac{\partial}{\partial y}\left(\kappa\left(T\right)\frac{\partial T}{\partial y}\right)+\mathrm{Br}\left[\frac{1}{1+\lambda_1}\left(\frac{\partial^2\psi}{\partial y^2}\right)^2+M^2\sin^2\phi\left(\frac{\partial\psi}{\partial y}+1\right)^2\right]=0, \tag{31}$$

where

$$\kappa(T)=1+\epsilon T. \tag{32}$$

3. Boundary conditions

The appropriate dimensionless velocity slip conditions can be expressed as

$$\begin{cases}\psi &= \frac{F}{2},\ \ \frac{\partial\psi}{\partial y}+\beta_1\frac{\partial^2\psi}{\partial y^2}=-1,\ \ \text{at}\ \ y=h_1\left(x\right),\\ \psi &= -\frac{F}{2},\ \ \frac{\partial\psi}{\partial y}-\beta_1\frac{\partial^2\psi}{\partial y^2}=-1,\ \ \text{at}\ y=h_2\left(x\right).\end{cases} \tag{33}$$

The temperature jump conditions are defined as

$$\begin{cases}T+\beta_2\frac{\partial T}{\partial y}=0,\ \ \text{at}\ \ y=h_1\left(x\right),\\ T-\beta_2\frac{\partial T}{\partial y}=1,\ \ \text{at}\ \ y=h_2\left(x\right).\end{cases} \tag{34}$$

In above equation, β_1 is the velocity slip parameter, whereas, β_2 is the thermal slip parameter.

4. Method

Taking cross differentiation of Eqs (29) and (30), we arrive at

$$0 = \frac{\partial^2}{\partial y^2}\left(\frac{1}{1+\lambda_2}\frac{\partial^2 \psi}{\partial y^2}\right) - M^2 \sin^2\phi\left(\frac{\partial^2 \psi}{\partial y^2}\right). \tag{35}$$

The general solution of Eq. (35) is

$$\psi(x,y) = D_1 + D_2 y + D_3 \cosh\left[M\sin\phi\sqrt{1+\lambda_2}y\right] + D_4 \sinh\left[M\sin\phi\sqrt{1+\lambda_2}y\right], \tag{36}$$

where D_1, D_2, D_3 and D_4 are constants. The constants are obtained using boundary condition (33). The axial pressure gradient has been obtained as

$$\frac{dp}{dx} = -\frac{D_5 D_6 + D_7}{R_{11} + R_{12} + R_{13}R_{14}}. \tag{37}$$

Since Eq. (31) is highly non linear, so it is difficult to find the analytical solution. In this study, a perturbation technique has been used to calculate the temperature distribution of Jeffery fluid, so we construct perturbation solution for a small ε as

$$T(x,y) = T^{(0)}(x,y) + \varepsilon T^{(1)}(x,y), \tag{38}$$

where $(0 < \varepsilon < 1)$.

Using Eq. (38) into Eqs (31) and (34) give yield zeroth order and 1st order systems of the temperature distribution, correspondingly. These are given by

Zeroth order system

$$\frac{\partial^2 T^{(0)}}{\partial y^2} + \mathrm{Br}\left[\frac{1}{1+\lambda_1}\frac{\partial^2 \psi}{\partial y^2} + M^2\sin^2\phi\left(\frac{\partial \psi}{\partial y}+1\right)^2\right] = 0, \tag{39}$$

$$\begin{cases} T^{(0)} + \beta_2 \frac{\partial T^{(0)}}{\partial y} = 0, & \text{at } y = h_1(x), \\ T^{(0)} - \beta_2 \frac{\partial T^{(0)}}{\partial y} = 1, & \text{at } y = h_2(x). \end{cases} \tag{40}$$

First order system

$$\frac{\partial^2 T^{(1)}}{\partial y^2} + \frac{\partial}{\partial y}\left(T^{(0)}\frac{\partial T^{(0)}}{\partial y}\right) = 0, \tag{41}$$

$$\begin{cases} T^{(1)} + \beta_2 \frac{\partial T^{(1)}}{\partial y} = 0, & \text{at } y = h_1(x), \\ T^{(1)} - \beta_2 \frac{\partial T^{(1)}}{\partial y} = 1, & \text{at } y = h_2(x). \end{cases} \tag{42}$$

Solving zeroth and first order systems, we find that

$$T^{(0)} = -f_0(x,y) + D_8 y + D_9, \tag{43}$$

$$T^{(1)} = -f_1(x,y) + D_{10} y + D_{11}. \tag{44}$$

The heat transfer coefficient defined as

$$Z = \frac{\partial h_2}{\partial x} \times \frac{\partial T}{\partial y}. \tag{45}$$

5. Graphical illustrations

This section is aimed to study the slip effects and their importance on a peristaltic mechanism under the influence of different emerging parameters. The graphs have been drawn for various concerned parameters. Note that the values of the parameters are fixed as $s_1 = 0.75$, $s_2 = 0.75$, $\eta = 1$, $\theta = \pi/4$ for all graphs and Tables.

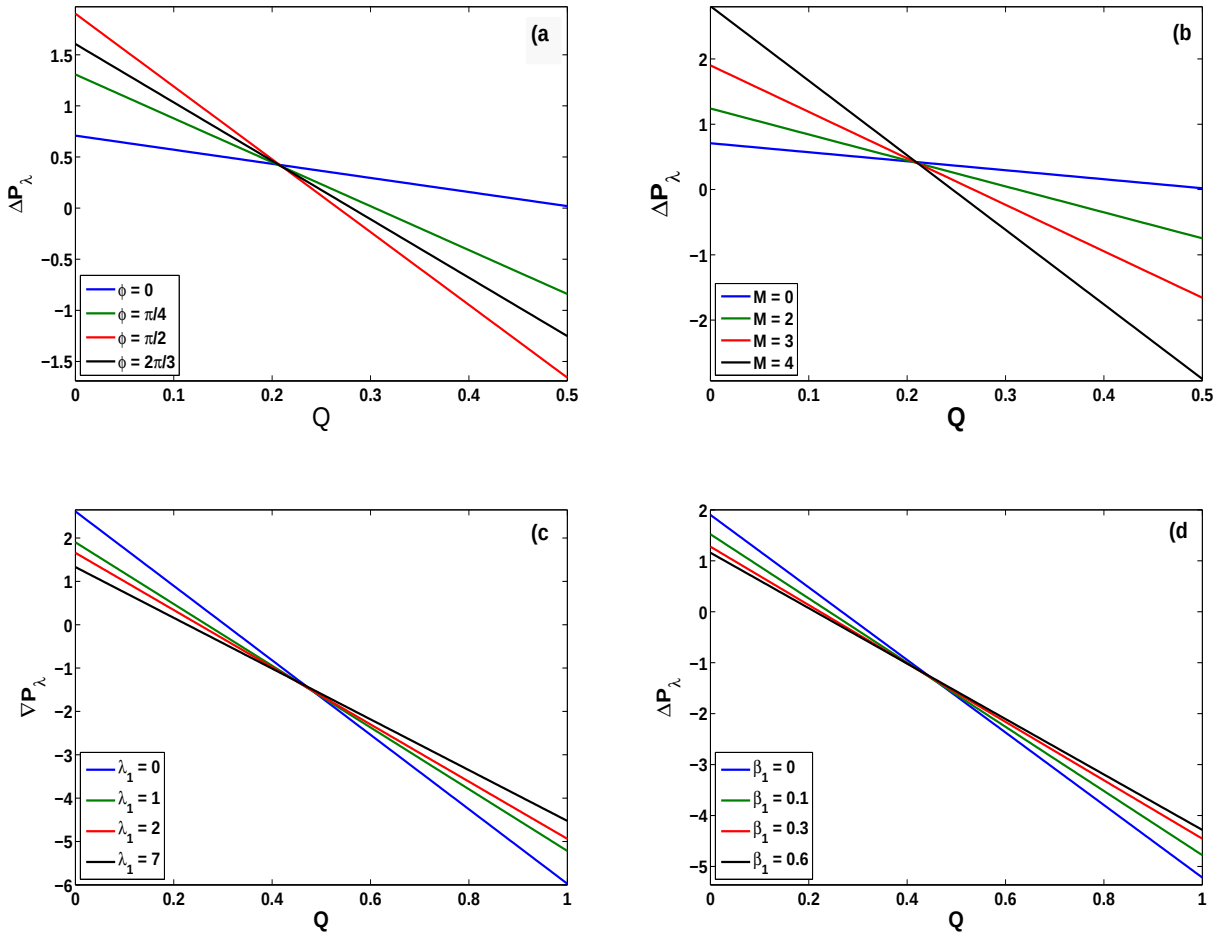

Figure 2. Pressure drop ΔP_λ vs Q for (a): $M = 4$, $\lambda_1 = 1$,$\beta_1 = 0.2$, (b): $\phi = \pi/4$,$\beta_1 = 0.2$, $\lambda_1 = 1$, (c): $\phi = \pi/4$,$\beta_1 = 0.2$, $M = 1$, (d): $M = 4$, $\lambda_1 = 1$,$\phi = \pi/4$.

5.1. Pumping features

The variation of pressure drop per wavelength ΔP_λ verses flow rate Q is shown in Figure 2. Influence of inclination angle ϕ on pressure drop ΔP_λ is depicted in Figure 2(a). It is observed that In the peristaltic pumping region, the pumping rate starts increasing when ϕ is increased from 0 to $\pi/2$; whereas it decreases in the augmented pumping region. It shows opposite behavior for $\phi \in [0, \pi/2]$. Figure 2(b) give us opportunity to study the connection between Hartman number M and ΔP_λ. In the positive feasible solution area which is the peristaltic pumping area, a rise in pressure drop is observed as we increase Heartman number M. In the augmented pumping region action of pumping performance remains increasing. Figure 2(c) is papered to investigate the behavior on ΔP_λ by Jeffrey fluid parameter λ_1 . It is seen that the pumping rate under the effects of λ_1 shows increasing behavior. Figure 2(d) illustrate the effects of thermal slip parameter β_1 on $\Delta P_\lambda > 0$. It is seen that the pumping rate under the effects of λ_1 shows increasing behavior.

Figure 3 shows the pressure gradient profile for one wavelength. It illustrates that in the wider part of channel $x \in [0, 0.2]$ and $x \in [0.65, 1]$ the flow can pass easily without implementation of a large pressure

Table 1. Z (Heat transfer coefficient) as function of ϕ and ε. Here $x = 0.1$, $Q = -1.2$, $M = 4$, $\lambda_1 = 1$, Br $= 0.5$, $\beta_1 = 0.2$, $\beta_2 = 0.2$.

	ϕ				
ε	$\pi/4$	$\pi/2$	$2\pi/3$	$5\pi/6$	$7\pi/8$
0.0	1.6713	2.41269	2.04214	1.29947	1.14463
0.1	1.6961	2.41624	2.05731	1.33195	1.17971
0.2	1.7209	2.41979	2.07247	1.36443	1.21479

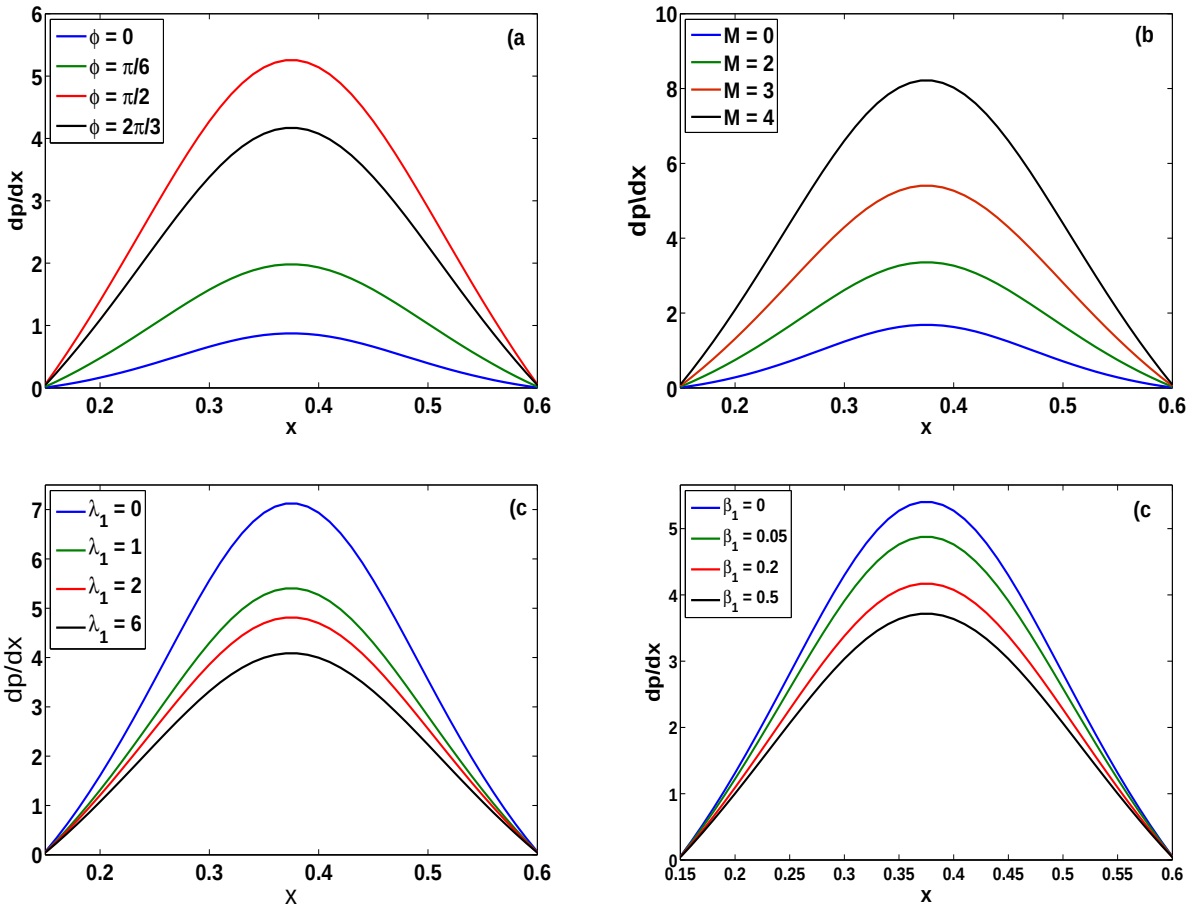

Figure 3. dp/dx (pressure gradient) vs $x \in [-0.5, 0.5]$ for $Q = 0.1$, (a): $M = 4$,$\beta_1 = 0.2$, $\lambda_1 = 1$, (b): $\phi = \pi/4$, $\beta_1 = 0.2$, $\lambda_1 = 1$, (c): $\phi = \pi/4$,$\beta_1 = 0.2$, $M = 4$, (d): $M = 4$, $\lambda_1 = 1$, $\phi = \pi/4$.

gradient, that's why pressure gradient is small in that region, but in the narrow part of the channel $x \in [0.3, 0.6]$, flow can pass with same flux under the large pressure gradient, especially the narrowest position $x = 0.45$. This phenomenon is well in accordance with the physical situation. We also observe the effect of ϕ, M, λ_1 and β_1 on dp/dx by using fixed values of other parameters. The amplitude of dp/dx increases with increase in values of ϕ and M while it decrease as λ_1 and β_1 increases.

The velocity profile for different parameters is shown in Figure 4. We observe that the velocity profile shows decreasing behavior for a gradually increase in ϕ, M, λ_1 and β_1.

5.2. Heat transfer characteristics

Figure 5 shows the variation of fluid temperature for various parameters. After examining Figure 5 we concluded that, if ϕ is raised from 0 to $\pi/2$ then temperature increases. As ϕ is raised from $\pi/2$ to π then temperature decreases. When Heartman number M is increased then the temperature is also increased, while an increase in λ_1 the temperature shows decreasing behavior. Under the effects of viscous and Joule

Table 2. Z (Heat transfer coefficient) as function of M and ε. Here $x = 0.1$, $Q = -1.2$, $\beta_1 = 0.2$, $\beta_2 = 0.2$, $\phi = \pi/4$, $\lambda_1 = 1$, Br $= 0.5$.

	M				
ε	1	2	3	4	5
0.0	0.97064	1.11242	1.34606	1.67129	2.08847
0.1	1.00824	1.14800	1.37690	1.69610	2.10229
0.2	1.04583	1.18358	1.40931	1.72090	2.11611

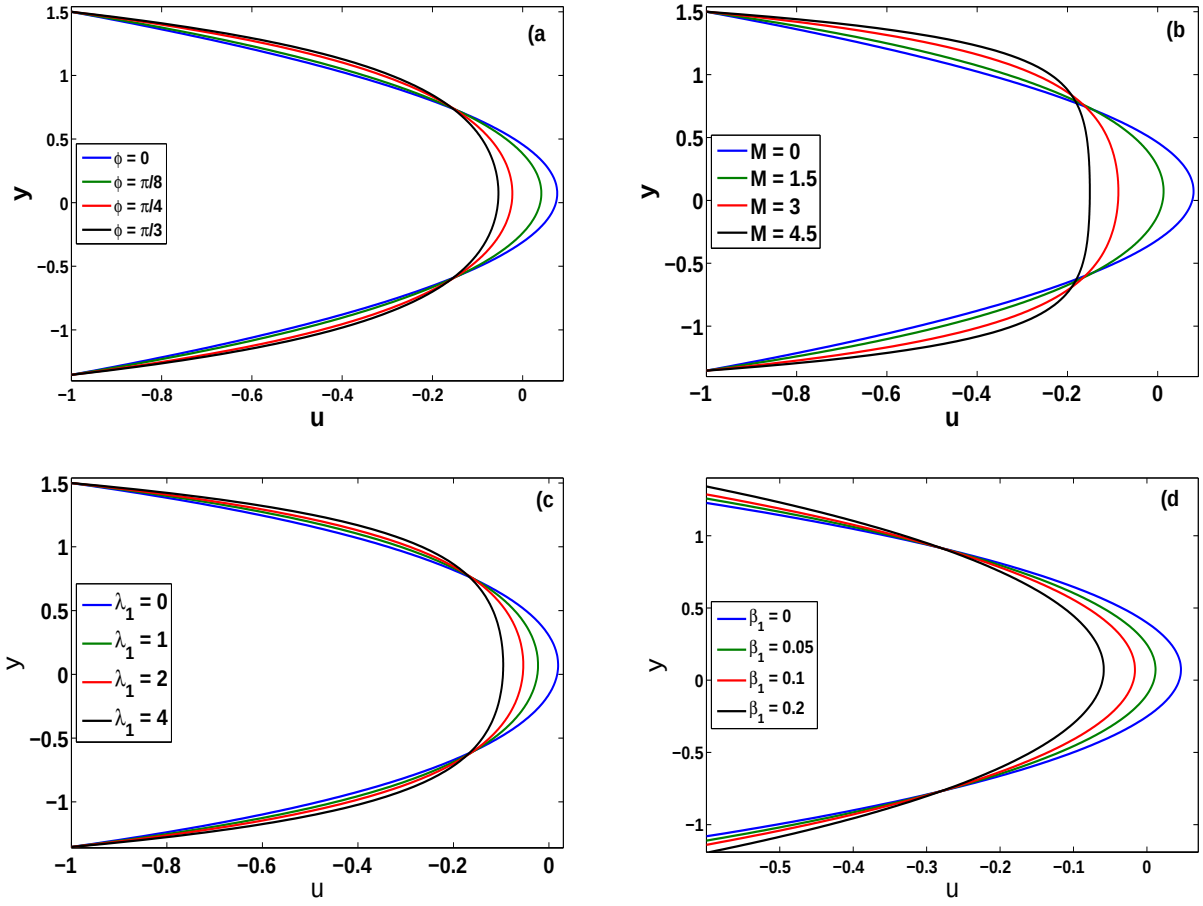

Figure 4. Distribution of velocity(u) vs y for $x = 0$, $Q = 1.2$, (a): $M = 4$,$\beta_1 = 0.2$ $\lambda_1 = 1$, (b): $\phi = \pi/4$,$\beta_1 = 0.2$, $\lambda_1 = 1$, (c): $\phi = \pi/4$, $\beta_1 = 0.2$, $M = 4$,(d): $M = 4$, $\lambda_1 = 1$, $\phi = \pi/4$.

dissipation, the temperature got increases with an increase in Br. An increase in thermal slip parameters and velocity slip parameter temperature shows decreasing behavior.

Tables 1-6 give us the numerical results of heat transfer coefficient Z various parameters. From Table 1, we observe that the heat transfer coefficient is less for hydrodynamic fluid but large for the hydromagnetic fluid. The value of the heat transfer coefficient Z increases under the effect of $\phi \in [0, \pi/2]$; however, opposite behavior is observed for $\phi \in [\pi/2, \pi]$. Table 2 tells us that the value of Z increases as we move from Jeffrey fluid to Newtonian fluid. Table 4 witness that the heat transfer coefficient Z increases under the consideration of the viscous and Joule dissipation. Table 5 and Table 6 tell us that the heat transfer coefficient Z decreases as we increase thermal slip parameters and velocity slip parameters.

5.3. Trapping phenomena

The plots for streamlines for different values of M, ϕ, β_1, β_2 and λ_1 are given in Figures 6-8. Figure 6 depicts that size of trapped bolus reduces as a result of increasing $\phi \in [0, \pi/2]$; however, the situation is reversed for $\phi \in [\pi/2, \pi]$, it displays an inverse behavior. Figure 7 concludes that the trapped bolus is smaller in size for hydromagnetic fluids than hydrodynamic fluids. It can be seen from Figure 8 that the size of the bolus is a decreasing function of Jeffrey fluid parameter λ_1. Figure 9 tells us that the size of the trapped bolus falls down with an increment in the value of velocity slip parameter β_1.

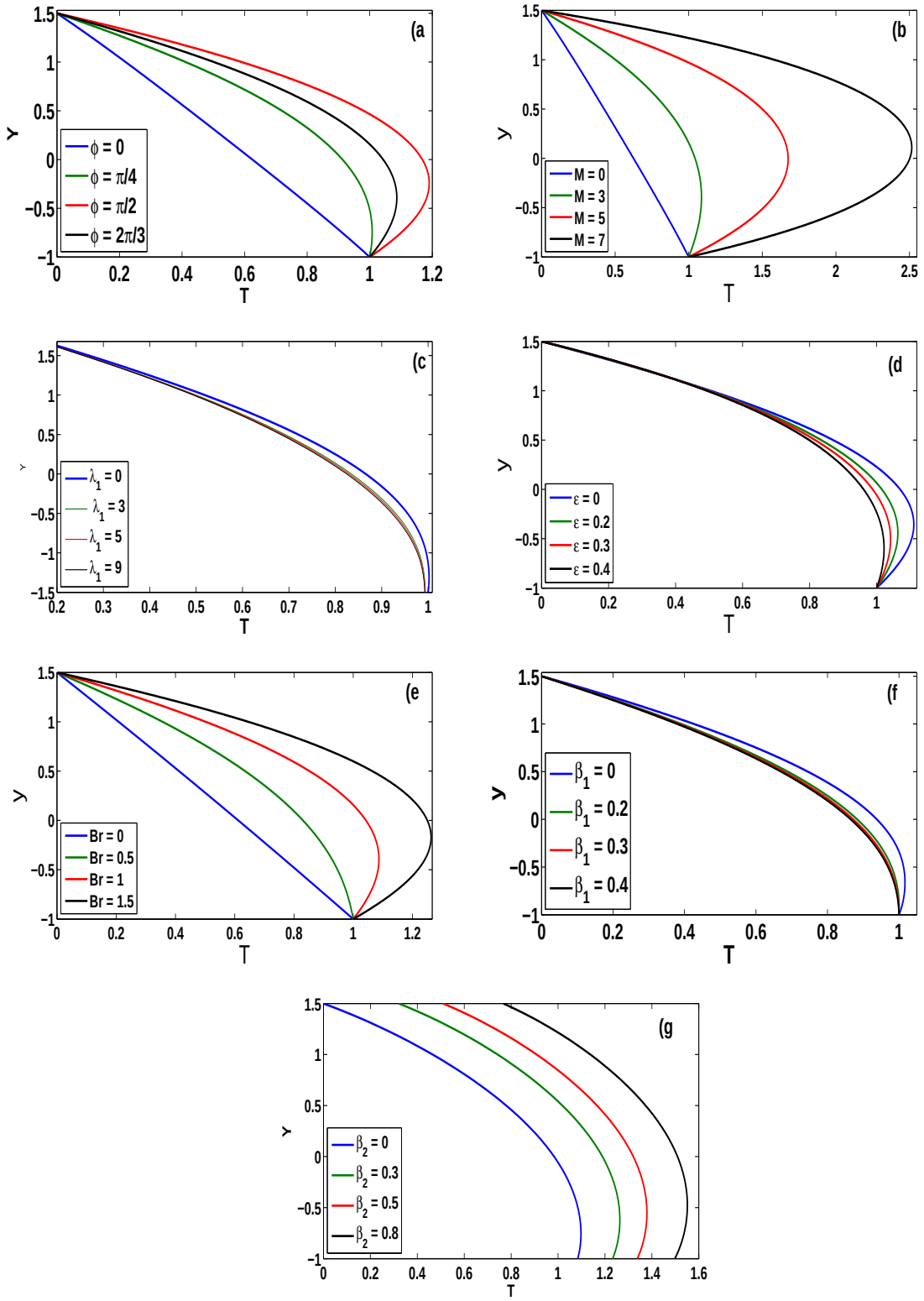

Figure 5. Distribution of temperature(T) vs y for $x = 0$, $Q = -1.2$, (a): $\varepsilon = 0.1$, $M = 4$, $\lambda_1 = 1$, $\beta_1 = 0.2$, $\beta_2 = 0.2$ Br $= 1$, (b): $\varepsilon = 0.1$, $\phi = \pi/4$,$\beta_1 = 0.2$, $\beta_2 = 0.2$, $\lambda_1 =$ Br $= 1$, (c): $\phi = \pi/4$, $M = 4$, Br $= 1.5$,$\beta_1 = 0.2$, $\beta_2 = 0.2$, $\varepsilon = 0.1$, (d): $\phi = \pi/4$, $M = 4$, Br $= 1$,$\beta_1 = 0.2$, $\beta_2 = 0.2$, (e): $\varepsilon = 0.1$, $\phi = \pi/3$,$\beta_1 = 0.2$, $\beta_2 = 0.2$, $M = 4$, $\lambda_1 = 1$, (f): $\varepsilon = 0.1$, $\phi = \pi/4$, $\lambda_1 =$ Br $= 1$.

Table 3. Z (Heat transfer coefficient) as a function of λ_1 and ε. Here $x = 0.1$, $Q = -1.2$, $\beta_1 = 0.2$, $\beta_2 = 0.2$, $\phi = \pi/4$, $M = 4$, Br $= 0.5$.

	λ_1				
ε	1	2	3	4	5
0.0	1.67129	1.65697	1.64965	1.64522	1.64226
0.1	1.69610	1.68210	1.67496	1.67063	1.66774
0.2	1.72090	1.70724	1.70026	1.69604	1.69321

Table 4. Z (Heat transfer coefficient) as a function of Br and ε. Here $x = 0.1$, $Q = -1.2$, $\beta_1 = 0.2$, $\beta_2 = 0.2$, $\phi = \pi/4$, $M = 4$, $\lambda_1 = 1$.

	Br				
ε	0.5	1	1.5	2	2.5
0.0	1.67129	2.45597	3.24064	4.02532	4.80999
0.1	1.69610	2.45803	3.21107	3.99555	4.69048
0.2	1.72090	2.46010	3.18151	3.88513	4.57098

Table 5. Z (Heat transfer coefficient) as a function of β_1 and ε. Here $x = 0.1$, $Q = -1.2$, $\beta_2 = 0.2$, $Br = 0.5$, $\phi = \pi/4$, $M = 4$, $\lambda_1 = 1$.

	β_1				
ε	0.1	0.2	0.3	0.4	0.5
0.0	1.70382	1.67129	1.65603	1.64778	1.64275
0.1	1.72792	1.69610	1.68124	1.67313	1.66822
0.2	1.75196	1.72090	1.70640	1.69848	1.69368

Table 6. Z (Heat transfer coefficient) as a function of β_2 and ε. Here $x = 0.1$, $Q = -1.2$, $\beta_1 = 0.2$, $Br = 0.5$, $\phi = \pi/4$, $M = 4$, $\lambda_1 = 1$.

	β_2				
ε	0.1	0.2	0.3	0.4	0.5
0.0	1.73194	1.67129	1.61795	1.57066	1.52845
0.1	1.76865	1.69610	1.63254	1.57635	1.52629
0.2	1.80537	1.72090	1.64713	1.58205	1.52414

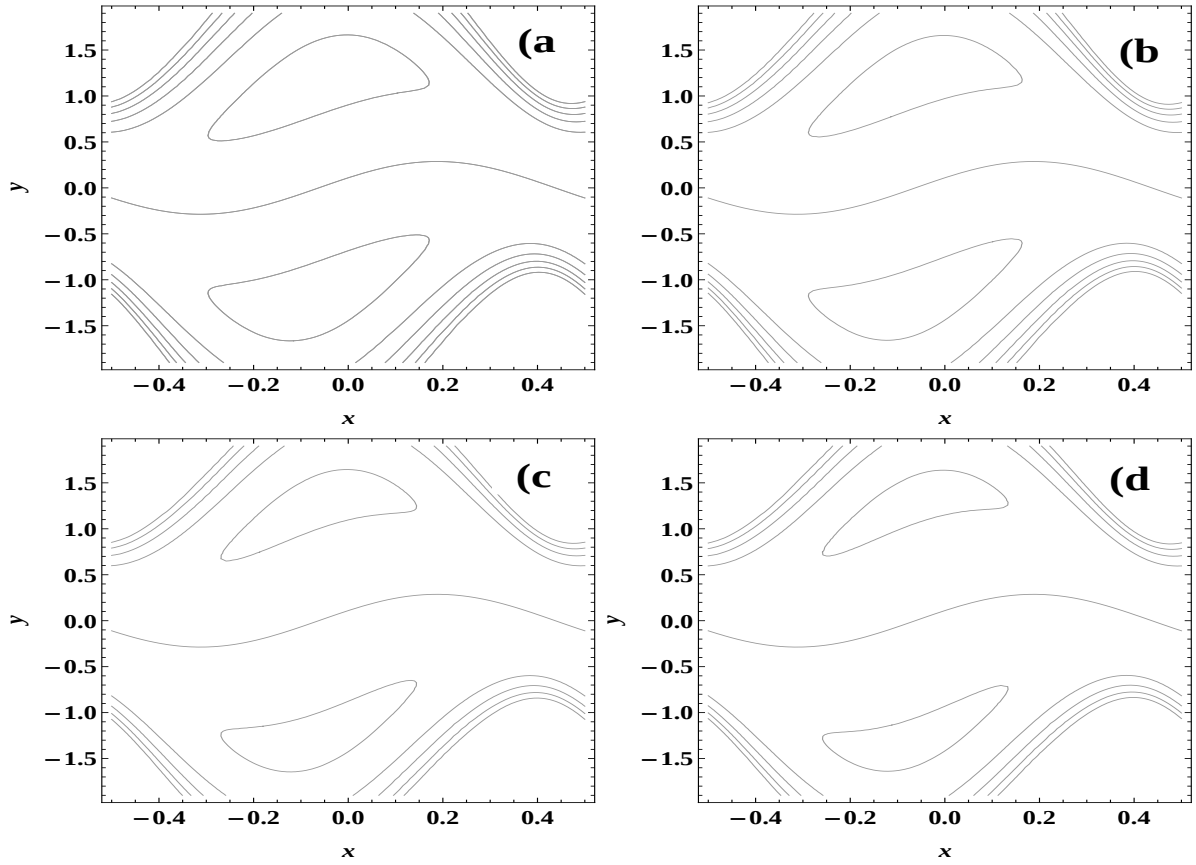

Figure 6. Effect on trapping by ϕ with $Q = 1.48$, $M = 1.2$, $\lambda_1 = 1$, (a); ϕ=0, (b); $\phi = \pi/6$, (c); $\phi = \pi/3$, (d); $\phi = \pi/2$.

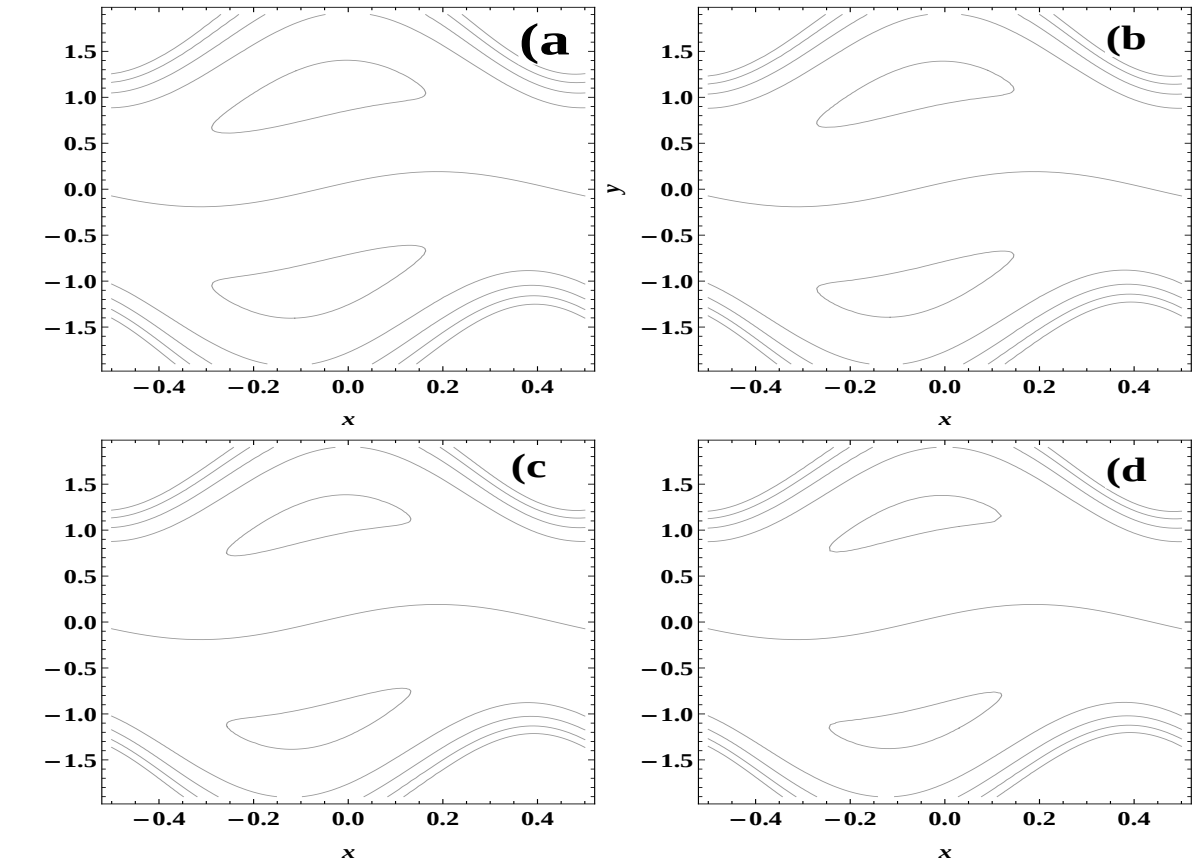

Figure 7. Effect on trapping by M with $Q = 1.48$, $\phi = \pi/4$, $\lambda_1 = 1$(a); M=0, (b); M=1, (c); M=1.3, (d); M=1.5 .

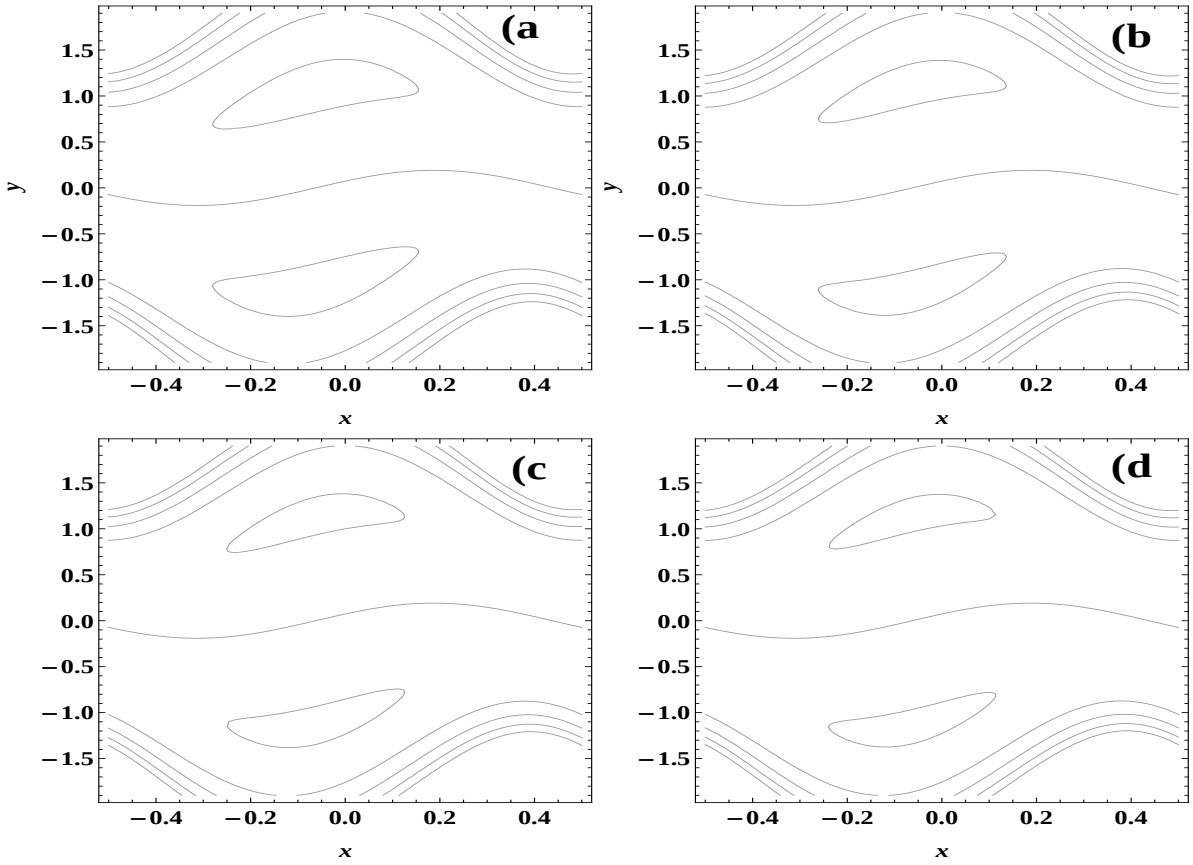

Figure 8. Influence of λ_1 on trapping with $Q = 1.48$, $\phi = \pi/4$, $M = 1$ (a); λ_1=0, (b); λ_1=2, (c); λ_1=3, (d); λ_1=4.

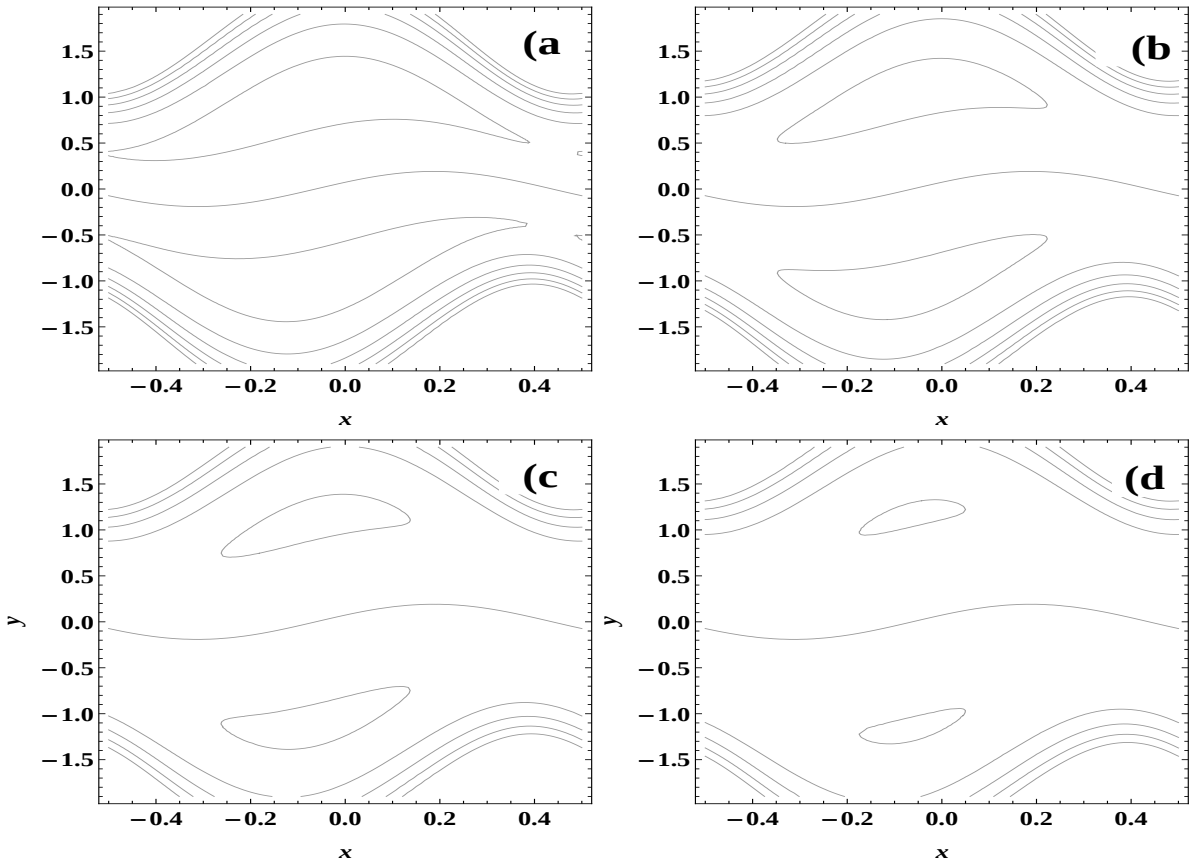

Figure 9. Effect on trapping by λ_1 with $Q = 1.48$, $\phi = \pi/4$, $M = 1$, $\lambda_1 = 1$ (a); β_1=0, (b); β_1=0.1, (c); β_1=0.2, (d); β_1=0.3, .

6. Concluding remarks

The peristaltic flow of a hydromagnetic Jeffrey fluid under the influence of an inclined magnetic field and variable thermal conductivity with slip conditions has been analyzed. The influence of various parameters is discussed graphically. The main finding can be summerize as listed below.

1. The magnetic field for$\phi \in [0, \pi/2]$ shows opposite behavior when compared with $\phi \in [\pi/2, \pi]$.
2. For magnetic fluid, the value of axial pressure gradient is higher rather than Newtonian fluid.
3. An increase in ϕ and M leads to an increase in dp/dx, whilst it decreases when λ_1 is increased.
4. The magnitude of dp/dx show decreasing behavior when β_1 is increased.
5. The amplitude of velocity u is a decreasing function of $\phi \in [0, \pi/2]$, β_1, M and λ_1.
6. The temperature of the fluid T falls down under the effect of $\phi \in [0, \pi/2]$; Contrarily, it decreases with an increase in conductivity parameter ε.
7. Ascending values of λ_1 decreases the value of heat transfer coefficient Z, whilst, an increment in the values of M, ε and Br leads to an increase in heat transfer coefficient Z.
8. The heat transfer coefficient decreases as we increase thermal slip parameters β_2 and velocity slip parameter β_1.
9. Size of the trapped bolus is greater for the inclined magnetic field as compared with the transverse magnetic field. Moreover, increasing M, β_1, and λ_1 decreases the size of the trapped bolus.

Appendix

Here we include the values of $D_i (i = 1, 2, ..., 11)$ and $R_i (i = 1, 2, .., 26)$.

$$
\begin{aligned}
R_1 &= 8(h_1 + h_2)\sqrt{1+\lambda_1},\\
R_2 &= \frac{R_1}{2}(-2 - FM^2\beta_1(1+\lambda_1) + FM^2\beta_1(1+\lambda_1)\cos 2\phi)\cosh((h_1 - h_2)M\sqrt{1+\lambda_1}\sin\phi),\\
R_{3a} &= M(1+\lambda_1)2(h_1 + h_2)(-4\beta_1 - F(2 + M^2\beta 1^2(1+\lambda_1),\\
R_{3b} &= FM^2\beta_1^2(1+\lambda_1)\cos 2\phi \sin\phi \sinh(M(\sqrt{1+\lambda_1})(h_1 - h_2)\sin\phi)),\\
R_4 &= -16\sqrt{1+\lambda_1},\\
R_{5a} &= 8\sqrt{1+\lambda_1}(2 - M^2\beta_1(h_1 - h_2)(1+\lambda_1) + (h_1 - h_2)M^2\beta_1(1+\lambda_1),\\
R_{5b} &= \cos 2\phi \cosh(M\sqrt{1+\lambda_1}\sin\phi(h_1 - h_2)),\\
R_{6a} &= 8M(1+\lambda_1)\sin\phi(h_1 - h_2 - 2\beta_1,\\
R_{6b} &= (h_1 - h_2)M^2\beta_1^2(1+\lambda_1)\sin\phi^2 \sinh(M\sqrt{1+\lambda_1}\sin\phi(h_1 - h_2))),\\
R_7 &= \cosh(h_1 M\sqrt{1+\lambda_1}\sin\phi)\sin\phi,\\
R_8 &= FM\sqrt{1+\lambda_1}\cosh(h2M\sqrt{1+\lambda_1}\sin\phi)FM\sqrt{1+\lambda_1}\sin\phi,\\
R_9 &= (2 + FM^2\beta_1(1+\lambda_1)\sin\phi^2),\\
R_{10} &= \sinh(\sqrt{1+\lambda_1}h1M\sin\phi) - \sinh(\sqrt{1+\lambda_1}\sin\phi h2M),\\
R_{11} &= \cosh(h1M\sqrt{1+\lambda_1}\sin\phi)\sin\phi,\\
R_{12} &= (h1 - h2)M\sqrt{1+\lambda_1}\cosh(h2M\sqrt{1+\lambda_1}\sin\phi)(h1 - h2)M\sqrt{1+\lambda_1}\sin\phi,\\
R_{13} &= -2 + (h1 - h2)M^2\beta 1(1+\lambda_1)\sin\phi^2,\\
R_{14} &= \sinh(\sin\phi h1M\sqrt{1+\lambda_1}) - \sinh(\sqrt{1+\lambda_1}h2M\sin\phi),\\
R_{15} &= \cosh(h_1 M\sqrt{1+\lambda_1}\sin\phi)(F + h_1 - h_2)\sqrt{1+\lambda_1},\\
R_{16} &= \cosh(h_2 M\sqrt{1+\lambda_1}\sin\phi)(F + h_1 - h_2),\\
R_{17} &= (F + h_1 - h_2)M\beta_1(1+\lambda_1)\sin\phi \sinh(h_1 M\sqrt{1+\lambda_1}\sin\phi),\\
R_{18} &= (F + h_1 - h_2)M\beta_1(1+\lambda_1)\sin\phi \sinh(h_2 M\sqrt{1+\lambda_1}\sin\phi),\\
R_{19} &= (h_1 - h_2)M^2\beta_1(1 + {\lambda_1}^3/2 + (1+\lambda_1)\cos 2\phi),\\
R_{20} &= \cosh(\sqrt{1+\lambda_1}\sin\phi(h_1 - h_2)M),\\
R_{21} &= (h_1 - h2)\sin\phi(2\beta_1 + M^2\beta_1^2(1+\lambda_1)\sin\phi^2)M(1+\lambda_1),\\
R_{22} &= \sinh(h_1 - h_2 M\sqrt{1+\lambda_1}\sin\phi),\\
R_{23} &= \sin\phi\beta_1 1 + \lambda_1 \cosh(h_1 M\sqrt{1+\lambda_1}\sin\phi)(F + h_1 - h_2)M(F + h_1 - h_2)M,
\end{aligned}
$$

$$
\begin{aligned}
R_{24} &= \sin\phi\cosh(h_2M\sqrt{1+\lambda_1}\sin\phi)(F+h_1-h_2),\\
R_{25} &= \sqrt{(1+\lambda_1)}\sinh(h_1M\sqrt{1+\lambda_1}\sin\phi)(F+h_1-h_2),\\
R_{26} &= \sinh(h_2M\sqrt{1+\lambda_1}\sin\phi)\sqrt{(1+\lambda_1)}(F+h_1-h_2),\\
D_1 &= -\frac{R_1+R_2+R_{3a}+R_{3b}}{R_4+R_{5a}+R_{5b}-R_{6a}-R_{6b}},\\
D_2 &= \frac{R_7+R_8+R_9R_{10}}{R_{11}+R_{12}+R_{13}R_{14}},\\
D_3 &= -\frac{R_{15}-R_{16}+R_{17}+R_{18}}{(R_{19}R_{20}-R_{21}R_{22})},\\
D_4 &= \frac{R_{23}+R_{24}+R_{25}-R_{26}}{(R_{19}R_{20}-R_{21}R_{22})},\\
D_5 &= 2(F+h_1-h_2)M^3\cosh((h_1-h_2)M\sqrt{1+\lambda_1}\sin\phi)\sin\phi^3,\\
D_6 &= \sqrt{1+\lambda_1}\cosh(\frac{1}{2}(h_1-h_2)M\sqrt{1+\lambda_1}\sin\phi),\\
D_7 &= M\beta_1 1+\lambda_1\sin\phi\sinh(\frac{1}{2}(h_1-h_2)M\sqrt{1+\lambda_1}\sin\phi),\\
D_8 &= \frac{-1+f_0(x,h_2)+f_0(x,h_1)+\beta_2\left(f\prime_0(x,h_2)+f\prime_0(x,h_1)\right)}{2\beta_2+h_1+h_2},\\
D_9 &= \frac{\beta_2+h_1+f_0(x,h_1)(\beta_2+h_2)+f_0(x,h_2)(\beta_2+h_1)-\beta_2(\beta_2+h_1)\left(f\prime_0(x,h_2)\right)}{2\beta_2+h_1+h_2}\\
&\quad+\frac{f\prime_0(x,h_1)(2\beta_2^2+\beta_2h_1+\beta_2h_2-\beta_2-h_1)}{2\beta_2+h_1+h_2},\\
D_{10} &= \frac{-f_1(x,h_2)+f_1(x,h_1)+\beta_2\left(f\prime_1(x,h_2)+f\prime_1(x,h_1)\right)}{2\beta_2+h_1-h_2},\\
D_{11} &= \frac{-f_1(x,h_1)(-1+2\beta_2+h_1-h_2)+f_1(x,h_2)+(f_1(x,h_2)}{2\beta_2+h_1-h_2}\\
&\quad-\frac{f\prime_1(x,h_1)(\beta_2h_1-\beta_2h_2+2\beta_2^2+\beta_2)+f\prime_1(x,h_2)}{2\beta_2+h_1-h_2}.
\end{aligned}
$$

Conflicts of Interest: The authors declare that they have no conflict of interest.

Data Availability: All data required for this research is included within this paper.

Funding Information: No funding is available for this research.

Author Contributions: Z.A. developed the theoretical formalism, performed the analytic calculations, numerical and graphical simulations. S.T. and R.A. contributed to the final version of the manuscript. All authors read and approved the final version of manuscript.

Bibliography

[1] Ali, N., Hayat, T., & Sajid, M. (2007). Peristaltic flow of a couple stress fluid in an asymmetric channel. *Biorheology, 44*(2), 125-138.

[2] El Misiery, A. E. M. (2002). Effects of an endoscope and generalized Newtonian fluid on peristaltic motion. *Applied Mathematics and Computation, 128*(1), 19-35.

[3] Sobamowo, M. G., Kamiyo, O. M., Yinusa, A. A., & Akinshilo, T. A. (2020). Magneto-squeezing flow and heat transfer analyses of third grade fluid between two disks embedded in a porous medium using Chebyshev spectral collocation method. *Open Journal of Mathematical Sciences, 4*, 305-322.

[4] Hayat, T., Kara, A. H., & Momoniat, E. (2003). Exact flow of a third-grade fluid on a porous wall. *International Journal of Non-Linear Mechanics, 38*(10), 1533-1537.

[5] Misra, S., Narender, G., & Govardha, K. Numerical solution of boundary layer flow of MHD nanofluid over a stretching surface with chemical reaction and viscous dissipation effects. *Open Journal of Mathematical Sciences, 3*, 289 – 299

[6] Fetecau, C., & Fetecau, C. (2005). Starting solutions for some unsteady unidirectional flows of a second grade fluid. *International Journal of Engineering Science, 43*(10), 781-789.

[7] Hayat, T., & Kara, A. H. (2006). Couette flow of a third-grade fluid with variable magnetic field. *Mathematical and Computer Modelling, 43*(1-2), 132-137.

[8] Khalique, C. M., Safdar, R., & Tahir, M. (2019). First analytic solution for the oscillatory flow of a Maxwells fluid with annulus. *Open Journal of Mathematical Sciences, 2*, 1-9.

[9] Farooq, M. U., Khan, M. S., & Hajizadeh, A. (2019). Flow of viscous fluid over an infinite plate with Caputo-Fabrizio derivatives. *Open Journal of Mathematical Sciences, 3*, 115-120.

[10] Ali, N., & Hayat, T. (2007). Peristaltic motion of a Carreau fluid in an asymmetric channel. *Applied Mathematics and Computation, 193*(2), 535-552.

[11] Ferraro, V. C., & Plumpton, C. (1966). *Introduction to Magneto–Fluid Mechanics, 2nd Edition.* Clarendon Press, Oxford.

[12] Stud, V. K., Sephon, G. S., & Mishra, R. K. (1977). Pumping action on blood flow by a magnetic field. *Bulletin of Mathematical Biology, 39*(3), 385-390.

[13] Mekheimer, K. S. (2004). Peristaltic flow of blood under effect of a magnetic field in a non-uniform channels. *Applied Mathematics and Computation, 153*(3), 763-777.

[14] Nadeem, S., & Akbar, N. S. (2009). Peristaltic flow of a Jeffrey fluid with variable viscosity in an asymmetric channel. *Zeitschrift für Naturforschung A, 64*(11), 713-722.

[15] Oldroyd, J. G. (1950). On the formulation of rheological equations of state. *Proceedings of the Royal Society of London. Series A. Mathematical and Physical Sciences, 200*(1063), 523-541.

[16] Larson, R. G. (2013). *Constitutive Equations for Polymer Melts and Solutions*: Butterworths series in chemical engineering. Butterworth-Heinemann.

[17] Rajagopal, K. R. (1993). Mechanics of non-Newtonian fluids. *Pitman Research Notes in Mathematics Series*, 129-129.

[18] Afsar Khan, A., Ellahi, R., & Vafai, K. (2012). Peristaltic transport of a Jeffrey fluid with variable viscosity through a porous medium in an asymmetric channel. *Advances in Mathematical Physics, 2012*, Article ID 169642. https://doi.org/10.1155/2012/169642.

[19] Hayat, T., Javed, M., & Ali, N. (2008). MHD peristaltic transport of a Jeffery fluid in a channel with compliant walls and porous space. *Transport in Porous Media, 74*(3), 259-274.

[20] Kothandapani, M., & Srinivas, S. (2008). Peristaltic transport of a Jeffrey fluid under the effect of magnetic field in an asymmetric channel. *International Journal of Non-Linear Mechanics, 43*(9), 915-924.

[21] Pandey, S. K., & Tripathi, D. (2010). Unsteady model of transportation of Jeffrey-fluid by peristalsis. *International Journal of Biomathematics, 3*(04), 473-491.

[22] Vajravelu, K., Sreenadh, S., & Lakshminarayana, P. (2011). The influence of heat transfer on peristaltic transport of a Jeffrey fluid in a vertical porous stratum. *Communications in Nonlinear Science and Numerical Simulation, 16*(8), 3107-3125.

[23] Raju, K. K., & Devanathan, R. (1972). Peristaltic motion of a non-Newtonian fluid. *Rheologica Acta, 11*(2), 170-178.

[24] Radhakrishnamacharya, G. (1982). Long wavelength approximation to peristaltic motion of a power law fluid. *Rheologica Acta, 21*(1), 30-35.

Nomenclature

$\bar{X}, \bar{Y}$	Dimensional form of X coordinate and Y coordinate in laboratory frame
$\bar{u}, \bar{v}$	Dimensional form of velocity components in wave frame
$\bar{x}, \bar{y}$	Dimensional form of x coordinate and y coordinate in wave frame
x, y	Dimensionless form of x coordinate and y coordinate in wave frame
u, v	Dimensionless form of velocity components in wave frame
$\bar{H}_1, \bar{H}_2$	Wall structures dimensional form in laboratory frame
h_1, h_2	Wall structures dimensionless form in wave frame
θ_1, θ_2	Wave amplitudes
s_1, s_2	Ratios of Amplitude
c	Wave speed
ℓ_1, ℓ_2	Channel widths
γ	Phase difference
η	Ratios of channel widths
λ	Wavelength
ϕ	Inclination angle of magnetic field
$\bar{t}$	Dimensional form of time
t	Dimensionless form of time
$\bar{P}$	Dimensional form of Pressure
p	Dimensionless pressure
ΔP_λ	Pressure drop per wavelength
ψ	Stream function
$\bar{Q}$	Rate of flow of volume
F	Instantaneous rate of flow of volume
$\bar{\mathbf{\alpha}}$	Extra stress tensor of Jeffrey fluid
$\bar{\mathbf{I}}$	Identity tensor
$\dot{r}$	First Rivilin Ericksen tensor of Jeffrey fluid
$\bar{J}$	Current density
$\vec{\mathbf{B}}_0$	Magnetic field
M	Hartman number
Br	Brinkman number
Re	Reynolds number
ρ	Fluid density
μ	Fluid viscosity
λ_1	Jeffrey fluid parameter
λ_2	Retardation time
β_1	Velocity slip parameter
β_2	Thermal slip parameter